CHEMISTRY

Selective dehydrogenation of small and large molecules by a chloroiridium catalyst

Kuan Wang[1]†, Lan Gan[1,2]†, Yuheng Wu[1], Min-Jie Zhou[1,3], Guixia Liu[1], Zheng Huang[1,2]*

The dehydrogenation of abundant alkane feedstocks to olefins is one of the mostly intensively investigated reactions in organic catalysis. A long-standing, pervasive challenge in this transformation is the direct dehydrogenation of unactivated 1,1-disubstituted ethane, an aliphatic motif commonly found in organic molecules. Here, we report the design of a diphosphine chloroiridium catalyst for undirected dehydrogenation of this aliphatic class to form valuable 1,1-disubstituted ethylene. Featuring high site selectivity and excellent functional group compatibility, this catalytic system is applicable to late-stage dehydrogenation of complex bioactive molecules. Moreover, the system enables unprecedented dehydrogenation of polypropene with controllable degree of desaturation, dehydrogenating more than 10 in 100 propene units. Further derivatizations of the resulting double bonds afford functionalized polypropenes.

INTRODUCTION

Olefins are ubiquitous as intermediates and reagents for the synthesis of commodity and fine chemicals (*1*). As a result, the dehydrogenation of vast alkane feedstocks and, more widely, alkyl groups directly to give olefins is a reaction with enormous potential applicability (Eq. 1) (*2*, *3*)

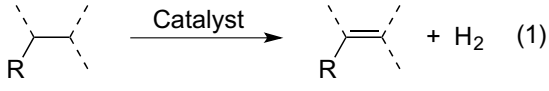

(1)

The yields and selectivity afforded by heterogeneous catalysts are generally very low, and the substrate scopes are limited to simple alkanes (e.g., ethane and propane), mainly due to harsh reaction conditions that the heterogeneous system requires (*4*). For this reason, the dehydrogenation using mild, reactive homogeneous organometallic systems is an area where the development of efficient and broadly applicable catalysts is highly desirable. One potential advantage that the milder organometallic system may have is the control of site selectivity. Because there are five classes of aliphatic substructures (beyond ethane) that can, in principle, be desaturated (Fig. 1A), the site selectivity is important but could be extremely difficult to achieve in complex or large molecules containing multiple desaturatable sites (see examples in Fig. 1B).

Pioneering works by Crabtree and co-workers (*5*, *6*) and Felkin and co-workers (*7*) have showed that monophosphine-ligated 14-electron Ir(I) fragments of the form of *trans*-L_2XM (**1**; L is a phosphine, and X is an anionic ligand; see Fig. 1C) are catalytically active for thermal transfer dehydrogenation (TD) of alkanes (i.e., using a hydrogen acceptor). Although groundbreaking, this system suffers from facile ligand degradation, thus severely limiting catalytic turnover (TO) numbers. Since then, many soluble transition metal catalysts have been developed for undirected alkane dehydrogenation (*8*–*17*). Among them, the most effective thermocatalytic system is that containing 14-electron (^{R}PCP)Ir fragments [**2**; ^{R}PCP is a bis(phosphino) aryl pincer ligand; R is substituents on the P atoms; see Fig. 1C] (*8*). For example, Goldman and co-workers (*10*) and this group (*14*) have showed that the *i*Pr-substituted pincer complexes with (^{iPr}PCP)Ir (**2c**) and ($^{iPr}P^{S}C^{O}P$)Ir (**2d**) fragments (see Table 1 for structures) could afford thousands of TOs in the TD of simple small alkanes. The (^{R}PCP)Ir system with a mer-type configuration shares the same symmetrical *trans*-L_2XM coordination geometry with Crabtree's monophosphine system: The anionic X ligand (which is an aryl group in the pincer) is trans to a vacant coordination site that is subject to substrate binding (Fig. 1C). The outperformance of the pincer complexes is in large part attributed to their high thermal stability (*8*). Nevertheless, the undirected dehydrogenation has been barely applied to organic synthesis because of low functional group tolerance and poor substrate scope (*18*). A key challenge limiting the scope and diversity is that the known reaction occurs effectively only with monosubstituted ethane (MSE) and 1,2-disubstituted ethane (1,2-DSE) (*8*). In contrast, the dehydrogenation of congested, unactivated 1,1-disubstituted ethane (1,1-DSE) has been exhibited with very scarce examples (*19*), and no examples of unactivated 1,1,2-trisubstituted ethane (1,1,2-TriSE) and 1,1,2,2-tetrasubstituted ethane (1,1,2,2-TetraSE) have been reported (Fig. 1A).

To broaden the applicability of the dehydrogenation chemistry, it is imperative to invent a broadly applicable catalyst for the desaturation of different aliphatic classes. The structural motif of 1,1-DSE is prevalent in natural and synthetic products [e.g., terpenoids and polypropene (PP); see Fig. 1B]. While directed dehydrogenation of 1,1-DSE using existing directing groups or pendant radical precursors (*20*–*23*) and dehydrogenation of activated 1,1-DSE (*24*–*26*) have been reported, methods of undirected dehydrogenation of unactivated 1,1-DSE have remained underexplored. In this work, we present the first examples of site-selective catalytic desaturation of unactivated 1,1-DSE to form 1,1-disubstituted ethylene without the need for a directing group. A diphosphine chloroiridium complex of the form of *cis*-L_2XM [which, contrasting with the classic *trans*-L_2XM type catalysts (*27*, *28*), has the anionic X ligand cis to the vacant coordination site; see **3** in Fig. 1C] was found to catalyze the TD of unactivated alkanes and aliphatics, including 1,1-DSE, with high selectivity and excellent functional group compatibility; the

[1]State Key Laboratory of Organometallic Chemistry, Shanghai Institute of Organic Chemistry, University of Chinese Academy of Sciences, Chinese Academy of Sciences, Shanghai 200032, China. [2]School of Chemistry and Material Sciences, Hangzhou Institute of Advanced Study, Hangzhou 310024, China. [3]Shenzhen Grubbs Institute and Department of Chemistry, Southern University of Science and Technology, Shenzhen 518055, China.
*Corresponding author. Email: huangzh@sioc.ac.cn
†These authors contributed equally to this work.

Table 1. Catalyst development for dehydrogenation of 1,1-DSE. Reaction conditions: catalyst (2 mol %), **4a** (0.2 mmol), TBE (0.2 mmol) in toluene-d8 (0.5 ml), 150°C, 1 hour. Yields were determined by ^{1}H NMR spectroscopy with CH_3NO_2 as the internal standard.

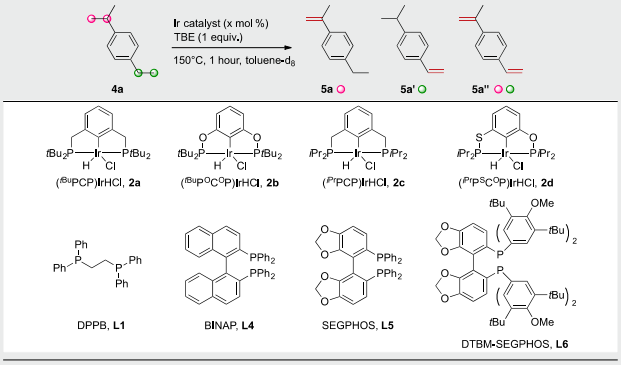

Entry	Ir catalyst (x mol % Ir)*	Additive (2x mol %)	Conv.	5a:5a′:5a″ (mol %)
1	**2a** (2% Ir)	NaO*t*Bu (4%)	2%	0:100:0
2	**2b** (2% Ir)	NaO*t*Bu (4%)	3%	0:100:0
3	**2c** (2% Ir)	NaO*t*Bu (4%)	19%	28:69:3
4	**2d** (2% Ir)	NaO*t*Bu (4%)	10%	5:95:0
5	1 **L1** + 0.5 $[Ir(COD)Cl]_2$ (2% Ir)	—	0%	—
6	1 **L4** + 0.5 $[Ir(COD)Cl]_2$ (2% Ir)	—	8%	59:35:6
7	1 **L5** + 0.5 $[Ir(COD)Cl]_2$ (2% Ir)	—	19%	65:30:5
8	1 **L6** + 0.5 $[Ir(COD)Cl]_2$ (2% Ir)	—	40%	83:12:5
9	1 **L6** + 0.5 $[Ir(COD)Cl]_2$ (10% Ir)	—	65%	75:10:15
10	2 PCy_3 + 0.5 $[Ir(COD)Cl]_2$ (2% Ir)	—	0%	—
11	2 PPh_3 + 0.5 $[Ir(COD)Cl]_2$ (2% Ir)	—	0%	—
12	1 **L6** + 0.5 $[Ir(COE)_2Cl]_2$ (2% Ir)	—	38%	82:10:8
13	1 **L6** + 0.5 $[Ir(COD)OMe]_2$ (2% Ir)	—	0%	—

*For entries 5 to 13 using the Ir dimer as the Ir source, *x* mol % Ir refers to the use of *x*/2 mol % Ir dimer and *x* mol % bidentate ligand or 2*x* mol % monodentate ligand.

synthetic application has been demonstrated by late-stage dehydrogenation of complex molecules and postfunctionalization of PP.

RESULTS

We embarked on our study with the identification of a catalyst for the TD of 1,1-DSE. An arene (**4a**) containing an isopropyl (1,1-DSE) and ethyl (MSE) groups para to each other was chosen as the model substrate for the purpose of assessing the site selectivity (Table 1). On the basis of the previous (^{R}PCP)Ir-catalyzed TD with *tert*-butylethylene (TBE) as the hydrogen acceptor, we initially examined the known pincer catalysts for the TD of **4a** with TBE (1 equiv.). With the *t*Bu-substituted complexes (^{tBu}PCP)IrHCl (**2a**) (*9*) and (^{tBu}P^{O}C^{O}P)IrHCl (**2b**) (*12*) as the precatalysts [2 mole percent (mol %)] and NaO*t*Bu as the catalyst activator, the reaction at 150°C gave low conversion after 1 hour, and the dehydrogenation occurred at the Et group (to form **5a′**) but not the *i*Pr group (entries 1 and 2). Under the same conditions, the runs using the less hindered, *i*Pr-substituted complexes **2c** and **2d** gave enhanced conversion (10 to 19%; entries 3 and 4). With **2d**, two products corresponding to the dehydrogenation of the *i*Pr (**5a**) and Et (**5a′**) groups, respectively, were observed (**5a**:**5a′** = 5:95). The reaction with **2c** afforded an additional product resulting from the double dehydrogenation of both the *i*Pr and Et groups (**5a″**). Although **5a′** was still the major product, the selectivity for **5a** was improved (**5a**:**5a′**:**5a″** = 28:69:3). These data suggest that the use of a less hindered pincer ligand favors the desaturation of the congested aliphatics.

However, earlier studies have shown that (^{R}PCP)Ir complexes with R smaller than *i*Pr tend to form catalytically inactive di- or multinuclear clusters (*29*). Considering this, we turned to bidentate diphosphine (P_2) ligands. The combination of such a ligand with an appropriate bite angle (~60° to 90°) and an X-type anionic ligand would generate a *cis*-P_2XIr fragment (*30*). The scaffold of *cis*-P_2XIr is expected to be more flexible than that of the isoelectronic (^{R}PCP)Ir ligated by rigid tridentate pincers. We envisioned that the employment of a sterically hindered bidentate ligand in *cis*-P_2XIr might be sufficient to offer protection against bimolecular catalyst deactivation or cluster formation, while the replacement of one bulky phosphine in *trans*-P_2XIr [or (^{R}PCP)Ir] at the position cis to the vacant coordination site with a sterically less demanding X ligand might favor the dehydrogenation of congested aliphatics (*29*).

With this in mind, a series of P_2 ligands were explored with $[Ir(COD)Cl]_2$ as the Ir source (using 2 equiv. of P_2 relative to $[Ir(COD)Cl]_2$; COD, cyclooctadiene). While the reaction with bis(diphenylphosphino)butane (DPPB) (**L1**) (entry 5), bis(diphenylphosphino)methane (DPPM) (**L2**), and bis(diphenylphosphino)ethane (DPPE) (**L3**) showed no activity (fig. S1), the run with 2,2′-bis (diphenylphosphino)-1,1′-binaphthyl (BINAP) (**L4**) gave 8% conversion. Despite the low activity, the site selectivity was promising, furnishing **5a** as the major product (**5a**:**5a′**:**5a″** = 59:35:6; entry 6). SEGPHOS (**L5**) afforded higher conversion (19%) and selectivity (**5a**:**5a′**:**5a″** = 65:30:5; entry 7). DTBM-SEGPHOS (**L6**) was found to be the most effective among the ligands investigated, giving **5a** with 83% selectivity at 40% conversion (entry 8). Increasing the loadings of the catalyst (10 mol % Ir) furnished 65% conversion, and the fraction of the double-dehydrogenation product **5a″** increased as expected (**5a**:**5a′**:**5a″** = 75:10:15; entry 9). The combination using a monophosphine ligand (4 equiv. PCy_3 or PPh_3 relative to $[Ir(COD)Cl]_2$) showed no activity (entries 10 and 11), presumably because of low thermal stability (*5*–*7*). The replacement of $[Ir(COD)Cl]_2$ with $[Ir(COE)_2Cl]_2$ [cyclooctene (COE)] had negligible impact on the reaction outcome (entry 12 versus 8), but the use of $[Ir(COD)OMe]_2$ was completely inactive for the dehydrogenation (entry 13).

The substrate scope of the TD reaction with an emphasis on illustrating the reactivity, compatibility, and site selectivity was then explored (Fig. 2). We first studied the catalytic activity of the **L6**/$[Ir(COD)Cl]_2$ combination (1 **L6** + 0.5 $[Ir(COD)Cl]_2$) in the benchmark reactions, the TD of *n*-octane, and cyclooctane with TBE (Fig. 2A). Heating the solution containing 20,000 *n*-octane:2000 TBE:1 Ir at 150°C gave octenes (**5b**) with 1020 TOs after 18 hours (see table S1 for product distribution). The catalytic efficiency and product selectivity are comparable to those obtained by the most effective pincer iridium catalysts (*10*, *14*). This catalyst also showed good activity for the conversion of cyclooctane to COE (**5c**), giving 357 TOs under the conditions used for *n*-octane.

With a focus of this study on the dehydrogenation of 1,1-DSE, we next investigated the reactivity of several small molecules of this class (Fig. 2A). For comparison, the reactions were conducted by using **L6**/$[Ir(COD)Cl]_2$, **2c**/NaO*t*Bu, and **2d**/NaO*t*Bu, respectively. Heating the solution containing 10,000 cumene (**4d**):1000 TBE:1 Ir at 150°C gave 980 TOs with **L6**/$[Ir(COD)Cl]_2$, 276 TOs with **2c**/NaO*t*Bu, and 68 TOs with **2d**/NaO*t*Bu after 18 hours. The dehydrogenation of a bulkier substrate, 1,1-diphenyl substituted ethane (**4e**), occurred at 150°C with **L6**/$[Ir(COD)Cl]_2$ using 2 mol % Ir and 1 equiv.

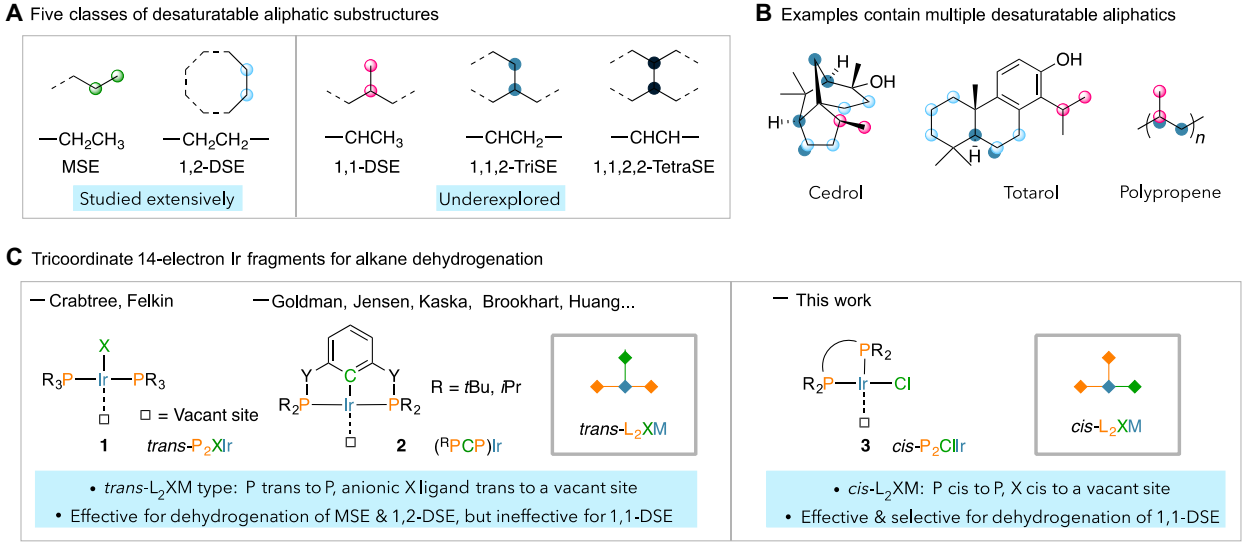

Fig. 1. Undirected catalytic dehydrogenation of various unactivated aliphatics. (**A**) Five classes of aliphatic substructures that are subject to desaturation to form olefins. (**B**) Representative examples contain multiple desaturatable aliphatic substructures. (**C**) Proposed tricoordinate 14-electron iridium species that are catalytically active for thermal alkane dehydrogenation.

TBE (relative to **4e**) in mesitylene and furnished the desaturated product **5e** in 51% yield after 4 hours. In contrast, the runs with **2c**/NaO*t*Bu or **2d**/NaO*t*Bu gave minimal conversion. **L6**/$[Ir(COD)Cl]_2$ is even effective for the desaturation of a highly congested, adamantyl-substituted 1,1-DSE (**4f**), whereas **2c**/NaO*t*Bu and **2d**/NaO*t*Bu are completely inactive in this case. The dehydrogenation of 2,4-dimethyl-pentane (**4g**) with **L6**/$[Ir(COD)Cl]_2$ afforded two products, 1,1-disubstituted olefin **5g** and trisubstituted olefin **5g′**, in 43% combined yield after 4 hours with the former as the major product (**5g**:**5 g′** = 5.3:1). As a comparison, the pincer catalysts are hardly active toward **4g**. Since **4g** can be viewed as a model substrate of PP, these results suggest that the **L6**/$[Ir(COD)Cl]_2$ combination may hold promise for the dehydrogenation of this polymer class (vide infra). The superior performance of **L6**/$[Ir(COD)Cl]_2$ in the desaturation of 1,1-DSE was further demonstrated by the example of 2,4-diphenyl-pentane (**4h**). The reaction produced three products in 32% total yields: one 1,1-disubstituted olefin (**5h**) and two dienes (**5h′** and **5h″**) [**5h**:(**5h** + **5h′**) = 90:10], while only trace amounts of the dehydrogenation products were observed when **2c**/NaO*t*Bu or **2d**/NaO*t*Bu was used. Note that **L6**/$[Ir(COD)Cl]_2$ is inactive toward the more congested 1,1,2-triphenyl and 1,1,2,2-tetraphenyl substituted ethanes (**4i** and **4j**).

As aforementioned, one key issue of the undirected dehydrogenation reactions limiting their applications is the low functional group compatibility. In this context, we explored the dehydrogenation of 1-aryl, 1-methyl disubstituted ethanes bearing various functionalities on the aryl rings (Fig. 2B). To enhance the yields of desaturated products, the reactions were performed with 10 mol % catalyst (i.e., 10 mol % **L6** + 5 mol % $[Ir(COD)Cl]_2$) and 1.5 equiv. TBE (relative to the substrate) in mesitylene. Under these conditions, the dehydrogenation of **4d** gave 81% yield after 4 hours (**5d**), and the substrates with Me groups in the ortho, meta, and para positions of the aryl groups afforded similar yields (**5k** to **5m**). Various functional groups are well tolerated. The ether (**5n**), ester (**5o** and **5p**), and acetyl (**5q**) groups are compatible with the catalyst. The cyanide (**5r**) and thioether (**5s**) groups with fair coordination ability exert a notable impact on the dehydrogenation, but reasonable yields were still achieved. The catalyst tolerates an unprotected hydroxyl group in the ortho or para position of the aryl ring (**5t** and **5u**), although a carboxylic acid causes the catalyst poisoning (**5v**). The dehydrogenation of substrates bearing primary and secondary amines proceeded effectively (**5w** and **5x**). The F and Cl groups could be tolerated (**5y** and **5z**), but the reaction with Br- or I-containing substrate gave low or no conversion (**5aa** and **5ab**). 2-Benzylthiophene and 2-indole substituted aliphatics were dehydrogenated smoothly, showing the compatibility of this catalyst with heteroarenes (**5ac** and **5ad**). Moreover, the boron-substituted 1,1-DSE was desaturated to vinyl boronate ester (**5ae**) in high yield.

The site selectivity is critical in dehydrogenating molecules containing two or multiple inequivalent desaturatable aliphatics (Fig. 2C). This selective desaturation of the 1,1-DSE over the MSE moiety was observed for the pilot substrate **4a** using **L6**/$[Ir(COD)Cl]_2$ (vide supra). Monitoring the TD process revealed that the ratio of **5a**:**5a′** was 3.6:1 at the earliest time (3 min), and the ratios increased over time (e.g., 9.7:1 at 4 hours; see fig. S26 for more data). These results suggest a kinetic preference for the dehydrogenation of 1,1-DSE versus MSE, although the site selectivity for the disubstituted olefin could be enhanced by the thermodynamics of reversible hydrogenation (in accord with this hypothesis, submission of **5a′** to the catalytic conditions, but without TBE, resulted in the formation of **4a**, **5a**, and **5a″**; fig. S27).

To eliminate the potential effect of conjugation with the aryl ring on the site selectivity, we conducted the TD using 2-methyltridecane (**4af**) as the substrate. With a specific purpose to elucidate the selectivity between 1,1-DSE and MSE, the reaction was conducted at a relatively low temperature (at 110°C) to minimize the isomerization of the olefin products. The reactions with **L6**/$[Ir(COD)Cl]_2$ yielded 1,1-disubstituted olefin **5af** as the dominant product, along with multiple minor products including monosubstituted (**5af′**) and trisubstituted (**5af″**) olefins (Fig. 2C; see fig. S28 for more data), whereas the run with the pincer system **2d**/NaO*t*Bu under the otherwise identical conditions gave the monosubstituted olefin **5af′** as the major product at the early stages of the reaction (fig. S28) (*10*, *14*).

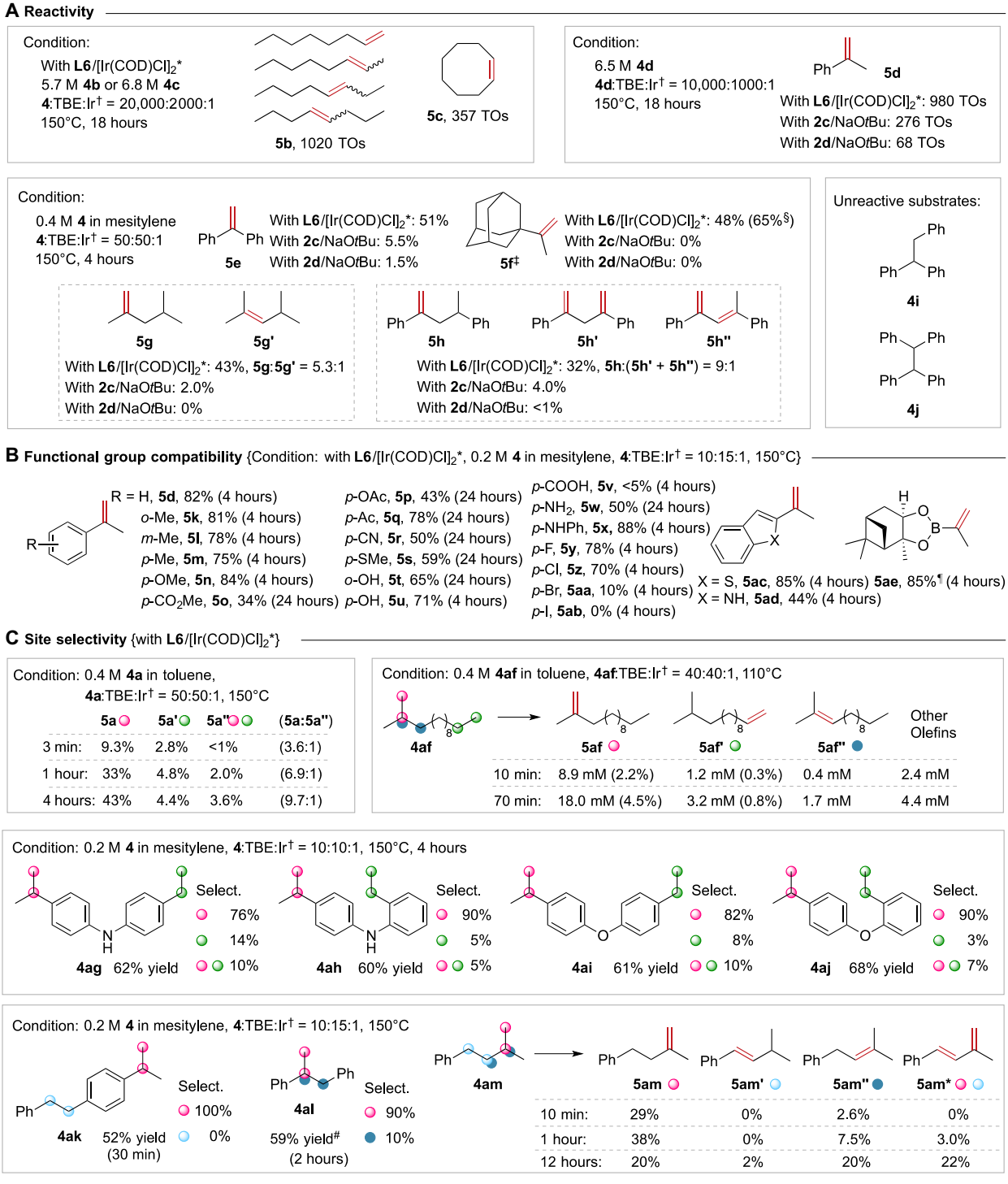

Fig. 2. Scope. (**A**) Reactivity of **L6**/[Ir(COD)Cl]$_2$ toward various aliphatic substructures. (**B**) Compatibility of **L6**/[Ir(COD)Cl]$_2$ toward various organic functional groups. (**C**) Site selectivity of **L6**/[Ir(COD)Cl]$_2$. Yields and TOs were determined by GC with internal standard unless otherwise noted. *__L6__/[Ir(COD)Cl]$_2$ = 1 **L6** + 0.5 [Ir(COD)Cl]$_2$. †The mole ratios refer to moles of Ir atom, not moles of the dimer [Ir(COD)Cl]$_2$. ‡The dehydrogenation of **4f** was conducted in toluene-d_8, and yields were determined by ^{1}H NMR with internal standard. §Using 1.5 equiv. of TBE relative to **4f** (0.4 M **4f** in toluene-d_8), **4f**:TBE:Ir = 50:75:1, 150°C, 4 hours. ¶Isolated yield. #Yield was determined by ^{1}H NMR with internal standard.

The selectivity for 1,1-DSE over MSE was further demonstrated by the reactions of diarylamines (**4ag** and **4ah**) and diarylethers (**4ai** and **4aj**) bearing *i*Pr and Et groups on two different aryl rings. All these reactions with **L6**/$[Ir(COD)Cl]_2$ afforded three products, two mono-dehydrogenation and one double-dehydrogenation products, among which the 1,1-DSE desaturation species (**5ag** to **5aj**) constituted the major products (76 to 90% selectivity).

In addition, the system **L6**/$[Ir(COD)Cl]_2$ exhibits excellent site selectivity for 1,1-DSE over 1,2-DSE. For example, the reaction of **4ak** produced 1,1-disubstituted ethylene exclusively (**5ak**, 52%), leaving the aryl-substituted 1,2-DSE untouched. The reaction of 1,2-diphenyl substituted propane (**4al**) furnished 53% 1,1-disubstituted (**5al**) and 6% trisubstituted olefin (**5al′**) after 2 hours. Monitoring the reaction for a longer period of time unveiled a **5al**-to-**5al′** conversion, albeit slowly (see table S2), indicating that the trisubstituted olefin was derived from the 1,1-disubstituted olefin via isomerization. The example of 1-Ph,3-Me butane (**4am**) is also illustrative as it contains a 1,2-DSE moiety between a 1,1-DSE and an aryl ring. 1,1-Disubstituted olefin was formed as the dominant product (**5am**) in the beginning (10 min), together with a small amount of trisubstituted olefin (**5am″**) stemming from the isomerization of **5am**; no product of direct dehydrogenation of the 1,2-DSE moiety (**5am′**) was observed. As the reaction proceeded, we observed the accumulation of a conjugated diene (**5am***), which was presumably produced via further dehydrogenation of the 1,2-DSE moiety in **5am** (in support of this hypothesis, submission of **5am** to the catalytic conditions formed **5am*** readily; see fig. S29). At the late stage of the reaction, we did observe a minimal amount of **5am′**, which was likely formed via hydrogenation of the 1,1-disubstituted olefin in **5am***, rather than direct dehydrogenation of **4am** (*31*).

With an understanding of the compatibility and site selectivity of this catalytic system, we evaluated the applicability of the TD reaction in more complex settings (Fig. 3A). Submission of guaiazulene, a natural product for anti-inflammation, to the catalytic conditions gave the desaturated product **5an** in high yield. The dehydrogenation of tubulin polymerization inhibitor produced 1,1-diarylethylene **5ao** in useful yield. The selective desaturation of the 1,1-DSE moiety in totarol proceeded effectively (**5ap**) despite the presence of multiple 1,2-DSE moieties and an *ortho*-OH group. The reaction of cedrol derivative is another example showing the exquisite site selectivity in complex settings: The 1,1-DSE moiety was desaturated preferentially over two 1,2-DSE and two 1,1,2-TriSE moieties, furnishing 1,1-dialkylethylene (**5aq**) in useful yield. 5-HT7 receptor inhibitor (**4ar**) contains two different desaturatable aliphatics, one 1,2-DSE between two N atoms and one 1,1-DSE. With **L6**/$[Ir(COD)Cl]_2$, the dehydrogenation occurred exclusively at the latter to form **5ar**. Such a site selectivity is complementary to that obtained by the photochemical dehydrogenation involving a hydrogen atom transfer mechanism (*26*), wherein the dehydrogenation occurred preferentially at the 1,2-DSE bearing the electron-rich C—H bonds adjacent to the N atoms (see fig. S30 for the comparative experiment).

The dehydrogenation of dehydroabietic acid derivatives has been investigated by Voica and co-workers (*20*) and Parasram and co-workers (*21*) independently: Using a guided desaturase, the reaction of dehydroabietyl amine derivative led to desaturation of the decalin system at the C2 and C3 positions (*20*), whereas the Pd-catalyzed visible light–induced dehydrogenation of dehydroabietol derivative occurred at the C6 and C7 positions (*21*). In contrast, treatment of dehydroabietic ester (**4as**) with this Ir catalyst resulted in selective formation of the 1,1-disubstituted olefin **5as** (Fig. 3A). These results highlight the potential applicability of the dehydrogenation chemistry for late-stage modification of complex molecules in a controlled and complementary fashion, editing structures with tailored C—C double-bond allocations.

In addition, the dehydrogenation-functionalization sequence with no need for purification of the olefin intermediates allowed for selective incorporation of the desired functionalities. For example, the bromomethoxylation of **5at** generated in situ from the TD of 2-*i*Pr–substituted naphthalene gave **6** in 81% isolated yield, and catalytic asymmetric hydroboration (*32*) and hydrosilylation (*33*) afforded the formal borylation (**7**) and silylation (**8**) products with high isolated yields and enantioselectivity. The dehydrogenation-hydroboration starting from **4au** furnished chiral alkyl boronate ester (**9**), which was oxidized to fenoprofen **10** with 97% enantiomeric excess (ee) and 54% total yield. Moreover, the dehydrogenation, coupled with isomerization, provides a previously unknown approach to stereodefined trisubstituted olefins (Fig. 3B). For example, the site-selective dehydrogenation of **4av** bearing a benzyl substituent yielded 1,1-disubstituted olefin **5av** as the dominate product, along with a trace amount of the trisubstituted olefin **11** (**5av**:**11** = 96:4; 56% combined yield). Using the Fe-catalyzed di-to-trisubstituted olefin isomerization (*34*), **5av** was converted to **11**, temarotene, with excellent stereoselectivity. (The trans configuration of the trisubstituted olefin was confirmed by x-ray diffraction.)

The chemoselective incorporation of functionalities into polyolefins can, to a great extent, improve their physical properties (*35*–*38*). Given the ability of **L6**/$[Ir(COD)Cl]_2$ to dehydrogenate the small-molecule **4g** (vide supra), we envisioned that this catalyst might catalyze the dehydrogenation of PP (Fig. 4A). Treatment of a PP [**12**, M_w = 28,400, PDI (polymer dispersity index) = 2.8] with **L6**/$[Ir(COD)Cl]_2$ (0.8 mol % Ir relative to the total amount of propene units) and TBE (0.10 M; propene unit:TBE = 8:1) in mesitylene at 150°C for 5 hours generated seven double bonds per 100 propene units (i.e., the level of desaturation was 7%), including 6 1,1-disubstituted olefins and 1 trisubstituted olefin (**13**). Under similar conditions, prolonging the reaction to 18 hours furnished 11 double bonds per 100 propene units with the di:trisubstituted olefin ratio being 3.5:1 (**14**). Using a higher–molecular weight (MW) PP (**15**; M_w = 362,400, PDI = 4.0), the reaction with TBE (0.10 M) after 1.5 hours formed two double bonds per 100 propene units with high selectivity for the disubstituted olefin (di:tri = 9:1; **16**). Doubling the loading of TBE (0.2 M) and prolonging the time (18 hours) produced the desaturated PP containing 12 double bonds per 100 propene units (di:tri = 4:1; **17**). These results indicate that the desaturation level can be controlled by the reaction time and the stoichiometry, and extending the time results in a higher fraction of trisubstituted olefins located in the polymer chain due to olefin isomerization.

GPC (gel permeation chromatography) analysis of the desaturated PPs (with the exception of **17**) showed no substantial changes in the MWs compared with the parent PPs, implying no chain cleavage or cross-linking. We hypothesized that the high olefin incorporation rate in the polymer chain of **17** might alter its conformation, thus affecting the GPC MW measurement. The hydrogenation of **17** yielded a PP **18** with MW comparable to the parent PP **15** (fig. S32). While the desaturated PPs **13** and **16** are white, the polymers **14** and **17** are light yellow, likely a result of the high-degree olefin incorporation. Note that the desaturation of PPs led to lower melting temperatures (if available) and improved solubility compared to parent PPs [e.g., **14** and **17** are even soluble in toluene at room temperature

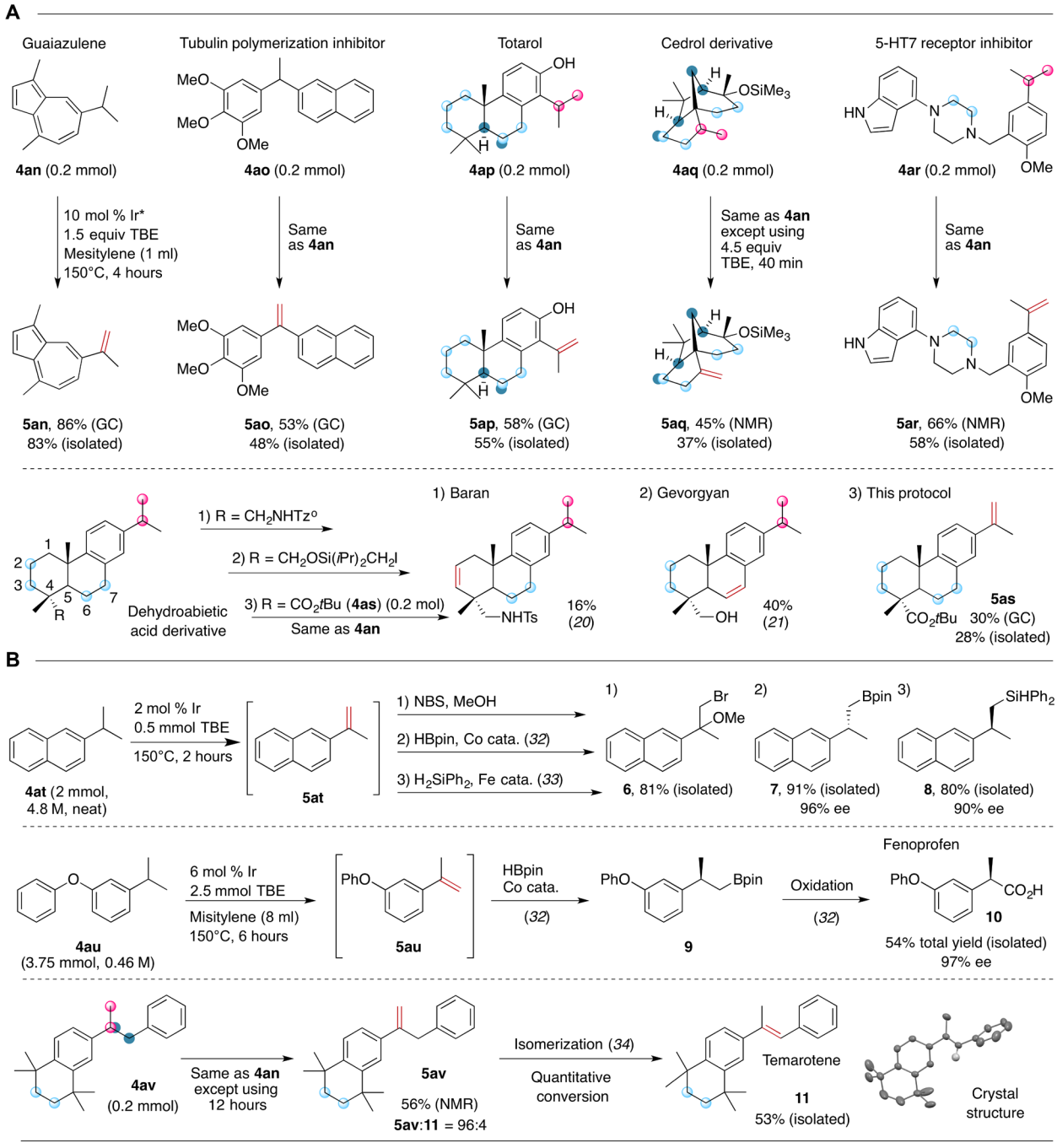

Fig. 3. Dehydrogenation in complex settings and derivatization of desaturated product. (**A**) Late-stage dehydrogenation of bioactive molecules. (**B**) Synthesis of fine chemicals and pharmaceutical ingredients via dehydrogenation. *"*x* mol % Ir" refers to the use of *x*/2 mol % $[Ir(COD)Cl]_2$ and x mol % DTBM-SEGPHOS (**L6**). cata., catalyst; Bpin, pinacolate boryl.

(RT)]. No melting transition was observed for **17**, and the high-degree incorporation of the double bonds into this high-MW PP yielded a polymer with elastic property (Fig. 4C; see movie S1 for the elastic behavior), which was neither observed for the lower–olefin incorporation variant **16** nor for the lower-MW variant **14** with similar olefin content.

The desaturated PPs can potentially undergo various functionalizations via derivatization of the resulting C─C double bonds (Fig. 4B). For example, the hydroxylation of **13** through a hydroboration-oxidation sequence resulted in the disappearance of all double bonds and the incorporation of 7 hydroxyls per 100 propene units, furnishing white, plate-shaped materials (**19**; Fig. 4C). The epoxidation of **13** occurred selectively at the less hindered 1,1-disubstituted olefins over the trisubstituted one, generating ca. five epoxides per 100 propene units (**20**). The characteristic signals for these functionalities were identified spectroscopically (see the Supplementary Materials). Again,

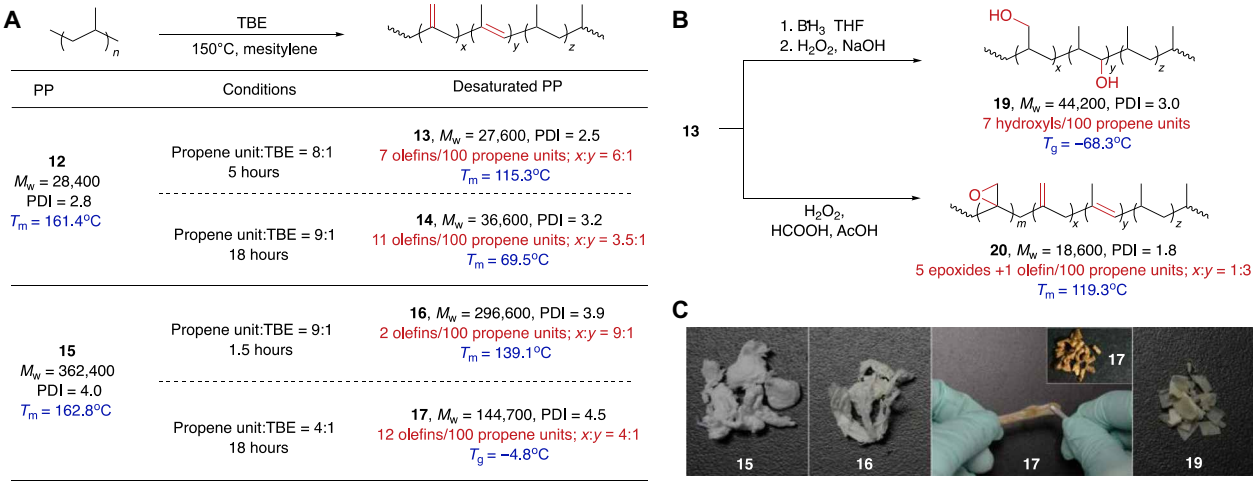

Fig. 4. Dehydrogenation of PP. (**A**) Dehydrogenation of two types of PPs with different MW. (**B**) Hydroxylation and epoxidation of the desaturated PP. (**C**) Polymeric materials of **15**, **16**, **17**, and **19**. T_m, melting temperature; T_g, glass transition temperature.

GPC analysis of the functionalized PPs showed no substantial changes in the MWs. The introduction of functionalities at a controllable level into the commodity PPs may create new approaches to preparing polymeric materials unattainable by conventional means (*39*, *40*).

Stoichiometric experiments were conducted to determine the potential catalytic intermediates (Fig. 5A). Reaction of $[Ir(COD)Cl]_2$ with DTBM-SEGPHOS (**L6**) in mesitylene at RT for 15 min formed a monomeric pentacoordinate complex (κ^2-P_2)IrCl(COD) (**21**) as the dominant species [90% nuclear magnetic resonance (NMR) yield; structure corroborated by NMR data]. Along with **21**, another species (**22**) was observed as well, albeit in very low yield (2%; see Fig. 5B for $^{31}P\{^1H\}$ NMR data). Heating the solution at 60°C for 9 hours resulted in the conversion of **21** to **22** as the major product (56%), and changing the reaction solvent to pentane allowed for the isolation of **22** in 70% yield. Although attempts to obtain x-ray quality crystals failed, the observation of a single ^{31}P NMR signal (Fig. 5B), together with mass and elemental analysis, establishes that **22** is a Cl-bridged dimeric complex $[(\kappa^2\text{-}P_2)IrCl]_2$ with a centrosymmetric structure (*41*).

Treatment of the isolated complex **22** with 1-octene formed an Ir(I) 1-octene adduct (**23**) (Fig. 5B), which has been previously crystallographically characterized, showing a square-planar geometry with the Cl ligand cis to the bound olefin (*42*). Moreover, **22** reacted with PhI to give a pentacoordinate Ir(III) phenyl iodo chloro complex **24**; x-ray diffraction analysis of **24** revealed a distorted trigonal bipyramid geometry, with Cl and one P atom at the axial positions (Fig. 5A). In contrast, the analogous Ir dimer $[(BINAP)IrCl]_2$ with the less hindered BINAP ligand (**L4**) is unreactive to 1-octene (see the Supplementary Materials for details), which appears to be inconsistent with a route that olefin addition precedes dimer cleavage. These observations imply that the dimeric complex **22** may break into a monomeric, tricoordinate Ir(I) species, *cis*-P_2ClIr (**3**) (Fig. 5A), which then undergoes the addition with olefin or PhI; apparently, the Cl group remains bound to the Ir, and the mer-type coordination geometry of the fragment *cis*-P_2ClIr is retained over the course of these addition reactions. Using **22** for the dehydrogenation of cumene (**4d**) afforded catalytic efficiency similar to that obtained by **L6**/$[Ir(COD)Cl]_2$ (see the Supplementary Materials). Collectively, these results suggest that the *cis*-P_2ClIr fragment **3** is the catalytically active species, which mediates alkane C—H bond addition to initiate the Ir(I)/Ir(III) dehydrogenation cycle (see fig. S34 for the proposed catalytic cycle) (*43*, *44*). Attempted synthesis of the hydride species by treatment of **L6**/$[Ir(COD)Cl]_2$ with $NaBEt_3H$ led to a product tentatively assigned as (**L6**)$IrH(L')_n$ (L′ is a neutral ligand) based on in situ NMR analysis, although further characterization was precluded because of low stability. The in situ formed species exhibited poor catalytic performance, suggesting that the hydride species is not likely a relevant on-cycle catalytic species (see the Supplementary Materials for details).

DISSCUSSION

The key difference between this *cis*-L_2XM and the traditional *trans*-L_2XM systems lies in the ligand arrangement: The vacant coordination site available for alkane C—H bond activation is cis to the X ligand in the former whereas trans in the latter. Seminal works by Krogh-Jespersen and co-workers (*45*) and Riehl and co-workers (*46*) have elucidated that the π-donation from the trans-X into the d orbital orthogonal to the P—Ir—P linkage has a favorable effect on the thermodynamics of alkane C—H addition (*47*). Thus, it is notable to note that the present *cis*-P_2ClIr system without the *trans*-X → Ir π-donation is effective for alkane dehydrogenation. With the *trans*-P_2ClIr systems, the alkane C—H addition (*29*, *43*, *44*) and the β-H elimination (BHE) step (*6*, *29*, *48*) both were found to be rate-determining of alkane dehydrogenation. It is our belief that the potentially unfavorable electronic effect in *cis*-P_2ClIr as a result of the lack of the *trans*-X → Ir π-donation could be outweighed by favorable steric effect. The substitution of one of the bulky phosphine groups in *trans*-P_2XIr with the small Cl group in *cis*-P_2ClIr, to a great extent, reduces the steric hindrance around the Ir center and would consequently lower the activation barrier for both the C—H addition and BHE steps (Fig. 5C). The steric contribution is expected to be particularly significant in the dehydrogenation of the relatively crowded 1,1-DSE. One possible explanation for the success of *cis*-P_2ClIr is that its ligand arrangement would allow for the formation of a favorable BHE transition state, in which the bulker substituent of 1,1-DSE is oriented toward

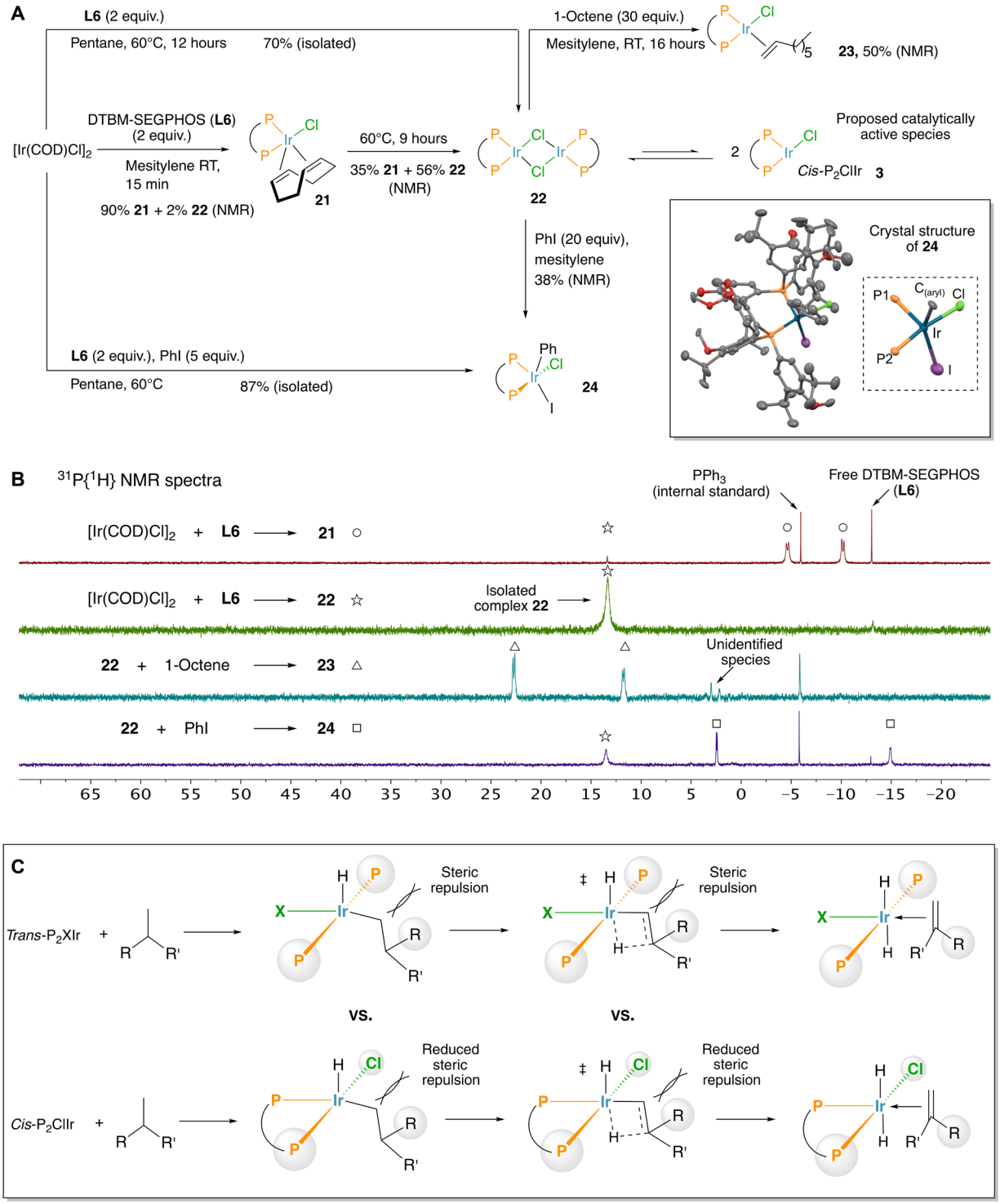

Fig. 5. Studies of the competent catalytic intermediates. (**A**) Synthesis of *cis*-P_2ClIr complexes. H atoms in the crystal structure of **24** were omitted for clarity. The inset only shows the Ir and the atoms bound to it. (**B**) $^{31}P\{^1H\}$ NMR stack plots. (**C**) Schematic illustration of the favorable steric effect of *cis*-P_2ClIr versus *trans*-P_2XIr on the C—H bond addition and BHE steps in the reaction with 1,1-DSE. R, large substituent; R′, small substituent.

the unbulky Cl group (Fig. 5C), although further computational and experimental studies are needed to provide insights into the origin of the reactivity. The design of organometallic catalysts of the form of *cis*-L_2XM for which the dehydrogenation could be applicable to more congested trisubstituted (1,1,2-TriSE) or tetrasubstituted ethane (1,1,2,2-TetraSE) is under way.

MATERIALS AND METHODS

Materials

Toluene and tetrahydrofuran were freshly distilled from sodium benzophenone ketyl before use. Mesitylene was distilled from $LiAlH_4$ and stored under argon. C_6D_6 and toluene-d_8 were dried under Na/K alloy and stored under argon. All other reagents and solvents used in this study were purchased from commercial sources and used as received unless otherwise stated.

Typical procedure for TD of small molecules

In an Ar-filled glove box, an oven-dried 10-ml thick-wall glass tube was charged with $[Ir(COD)Cl]_2$ (6.7 mg, 10 μmol, 5.0 mol %), DTBM-SEGPHOS (**L6**, 23.6 mg, 20 μmol, 10 mol %), cumene (**4d**, 24.0 mg, 0.2 mmol, 1.0 equiv.), TBE (39 μl, 0.3 mmol, 1.5 equiv.), and mesitylene (1.0 ml). The tube was sealed with a Teflon plug, and the reaction mixture was stirred at 150°C in a preheated oil bath for 4 hours. After that, the reaction was cooled to RT, and the resulting mixture was analyzed by gas chromatography (GC) with toluene as the internal standard (82% yield).

Typical procedure for dehydrogenation reaction of PP

In an Ar-filled glove box, an oven-dried 100-ml thick-wall glass tube was charged with $[Ir(COD)Cl]_2$ (67.2 mg, 0.1 mmol), DTBM-SEGPHOS (**L6**, 235.9 mg, 0.2 mmol), PP **12** (1.0 g), TBE (390 μl, 3 mmol, 0.1 M), and mesitylene (30.0 ml). The tube was sealed with a Teflon plug, and the reaction mixture was stirred at 150°C in a preheated oil bath for 5 hours. After that, the reaction mixture was poured into a flask containing cold methanol (−20°C). The precipitate was collected and then dried under reduced pressure to a constant weight to afford polymer PP **13** (980.0 mg).

SUPPLEMENTARY MATERIALS

Supplementary material for this article is available at https://science.org/doi/10.1126/sciadv.abo6586

REFERENCES AND NOTES

1. G. R. Lappin, L. H. Nemec, J. D. Sauer, J. D. Wagner, "[Olefins, Higher]" in *Kirk-Othmer Encyclopedia of Chemical Technology* (Wiley, 2010), pp. 1–20.
2. J. A. Labinger, J. E. Bercaw, Understanding and exploiting C–H bond activation. *Nature* **417**, 507–514 (2002).
3. R. G. Bergman, C–H activation. *Nature* **446**, 391–393 (2007).
4. J. J. H. B. Sattler, J. Ruiz-Martinez, E. Santillan-Jimenez, B. M. Weckhuysen, Catalytic dehydrogenation of light alkanes on metals and metal oxides. *Chem. Rev.* **114**, 10613–10653 (2014).
5. R. H. Crabtree, J. M. Mihelcic, J. M. Quirk, Iridium complexes in alkane dehydrogenation. *J. Am. Chem. Soc.* **101**, 7738–7740 (1979).
6. M. J. Burk, R. H. Crabtree, Selective catalytic dehydrogenation of alkanes to alkenes. *J. Am. Chem. Soc.* **109**, 8025–8032 (1987).
7. H. Felkin, T. Fillebeen-Khan, Y. Gault, R. Holmes-Smith, J. Zakrzewski, Activation of C-H bonds in saturated hydrocarbons. The catalytic functionalisation of cyclooctane by means of some soluble iridium and ruthenium polyhydride systems. *Tetrahedron Lett.* **25**, 1279–1282 (1984).
8. A. Kumar, T. M. Bhatti, A. S. Goldman, Dehydrogenation of alkanes and aliphatic groups by pincer-ligated metal complexes. *Chem. Rev.* **117**, 12357–12384 (2017).
9. M. Gupta, C. Hagen, R. J. Flesher, W. C. Kaska, C. M. Jensen, A highly active alkane dehydrogenation catalyst: stabilization of dihydrido rhodium and iridium complexes by a P–C–P pincer ligand. *Chem. Commun.* , 2083–2084 (1996).
10. F. Liu, E. B. Pak, B. Singh, C. M. Jensen, A. S. Goldman, Dehydrogenation of *n*-alkanes catalyzed by iridium "pincer" complexes: Regioselective formation of α-olefins. *J. Am. Chem. Soc.* **121**, 4086–4087 (1999).
11. K. Zhu, P. D. Achord, X. Zhang, K. Krogh-Jespersen, A. S. Goldman, Highly effective pincer-ligated iridium catalysts for alkane dehydrogenation. DFT calculations of relevant thermodynamic, kinetic, and spectroscopic properties. *J. Am. Chem. Soc.* **126**, 13044–13053 (2004).
12. I. Göttker-Schnetmann, P. White, M. Brookhart, Iridium bis(phosphinite) *p*-XPCP pincer complexes: Highly active catalysts for the transfer dehydrogenation of alkanes. *J. Am. Chem. Soc.* **126**, 1804–1811 (2004).
13. A. S. Alan, A. H. Roy, Z. Huang, R. Ahuja, W. Schinski, M. Brookhart, Catalytic alkane metathesis by tandem alkane dehydrogenation-olefin metathesis. *Science* **312**, 257–261 (2006).
14. W. Yao, Y. Zhang, X. Jia, Z. Huang, Selective catalytic transfer dehydrogenation of alkanes and heterocycles by an iridium pincer complex. *Angew. Chem. Int. Ed.* **53**, 1390–1394 (2014).
15. X. Jia, C. Qin, T. Friedberger, Z. Guan, Z. Huang, Efficient and selective degradation of polyethylenes into liquid fuels and waxes under mild conditions. *Sci. Adv.* **2**, e1501591 (2016).
16. J. A. Maguire, W. T. Boese, A. S. Goldman, Photochemical dehydrogenation of alkanes catalyzed by trans-carbonylchlorobis(trimethylphosphine)rhodium: Aspects of selectivity and mechanism. *J. Am. Chem. Soc.* **111**, 7088–7093 (1989).
17. A. D. Chowdhury, N. Weding, J. Julis, R. Franke, R. Jackstell, M. Beller, Towards a practical development of light-driven acceptorless alkane dehydrogenation. *Angew. Chem. Int. Ed.* **53**, 6477–6481 (2014).
18. X. Tang, L. Gan, X. Zhang, Z. Huang, *n*-Alkanes to *n*-alcohols: Formal primary C—H bond hydroxymethylation via quadruple relay catalysis. *Sci. Adv.* **6**, eabc6688 (2016).
19. Among the rare examples, the dehydrogenation occurred site-selectively at the 1,2-DSE of cycloalkane versus the 1,1-DSE; see Ref 6 and 16.
20. A.-F. Voica, A. Mendoza, W. R. Gutekunst, J. O. Fraga, P. S. Baran, Guided desaturation of unactivated aliphatics. *Nat. Chem.* **4**, 629–635 (2012).
21. M. Parasram, P. Chuentragool, Y. Wang, Y. Shi, V. Gevorgyan, General, auxiliary-enabled photoinduced Pd-catalyzed remote desaturation of aliphatic alcohols. *J. Am. Chem. Soc.* **139**, 14857–14860 (2017).
22. Y. Xia, K. Jana, A. Studer, Remote radical desaturation of unactivated C–H bonds in amides. *Chem. A Eur. J.* **27**, 16621–16625 (2021).
23. Z. Wang, L. Hu, N. Chekshin, Z. Zhuang, S. Qian, J. X. Qiao, J.-Q. Yu, Ligand-controlled divergent dehydrogenative reactions of carboxylic acids via C–H activation. *Science* **374**, 1281–1285 (2021).
24. Y. Izawa, D. Pun, S. S. Stahl, Palladium-catalyzed aerobic dehydrogenation of substituted cyclohexanones to phenols. *Science* **333**, 209–213 (2011).
25. J. G. West, D. Huang, E. J. Sorensen, Acceptorless dehydrogenation of small molecules through cooperative base metal catalysis. *Nat. Commun.* **6**, 10093 (2015).
26. M.-J. Zhou, L. Zhang, G. Liu, C. Xu, Z. Huang, Site-selective acceptorless dehydrogenation of aliphatics enabled by organophotoredox/cobalt dual catalysis. *J. Am. Chem. Soc.* **143**, 16470–16485 (2021).
27. Y. Segawa, M. Yamashita, K. Nozaki, Syntheses of PBP pincer iridium complexes: A supporting boryl ligand. *J. Am. Chem. Soc.* **131**, 9201–9203 (2009).
28. W.-C. Shih, O. V. Ozerov, Synthesis and characterization of PBP pincer iridium complexes and their application in alkane transfer dehydrogenation. *Organometallics* **36**, 228–233 (2017).
29. S. Kundu, Y. Choliy, G. Zhuo, R. Ahuja, T. J. Emge, R. Warmuth, M. Brookhart, K. Krogh-Jespersen, A. S. Goldman, Rational design and synthesis of highly active pincer-iridium catalysts for alkane dehydrogenation. *Organometallics* **28**, 5432–5444 (2009).
30. M.-N. Birkholz, Z. Freixa, P. W. N. M. van Leeuwen, Bite angle effects of diphosphines in C—C and C—X bond forming cross coupling reactions. *Chem. Soc. Rev.* **38**, 1099–1118 (2009).
31. An alternative approach to **5al'** involves further isomerization of **5al"**.
32. L. Zhang, Z. Zuo, X. Wan, Z. Huang, Cobalt-catalyzed enantioselective hydroboration of 1,1-disubstituted aryl alkenes. *J. Am. Chem. Soc.* **136**, 15501–15504 (2014).
33. J. Chen, B. Cheng, M. Cao, Z. Lu, Iron-catalyzed asymmetric hydrosilylation of 1,1-disubstituted alkenes. *Angew. Chem. Int. Ed.* **54**, 4661–4664 (2015).
34. S. Xu, G. Liu, Z. Huang, Iron catalyzed isomerization of α-alkyl styrenes to access trisubstituted alkenes. *Chin. J. Chem.* **39**, 585–589 (2021).
35. A. Bunescu, S. Lee, Q. Li, J. F. Hartwig, Catalytic hydroxylation of polyethylenes. *ACS Central Science* **3**, 895–903 (2017).
36. L. Chen, K. G. Malollari, A. Uliana, D. Sanchez, P. B. Messersmith, J. F. Hartwig, Selective, catalytic oxidations of C–H bonds in polyethylenes produce functional materials with enhanced adhesion. *Chem* **7**, 137–145 (2021).

37. R. Nakano, K. Nozaki, Copolymerization of propylene and polar monomers using Pd/IzQO catalysts. *J. Am. Chem. Soc.* **137**, 10934–10937 (2015).
38. M. Baur, F. Lin, T. O. Morgen, L. Odenwald, S. Mecking, Polyethylene materials with in-chain ketones from nonalternating catalytic copolymerization. *Science* **374**, 604–607 (2021).
39. A. Nakamura, S. Ito, K. Nozaki, Coordination–insertion copolymerization of fundamental polar monomers. *Chem. Rev.* **109**, 5215–5244 (2009).
40. E. Y.-X. Chen, Coordination polymerization of polar vinyl monomers by single-site metal catalysts. *Chem. Rev.* **109**, 5157–5214 (2009).
41. T. Y. Yamagata, A. Iseki, K. Tani, Preparation, properties and structures of $[IrCl(diphosphine)]_2$ (diphosphine = (*R*)-BINAP and BPBP). *Chem. Lett.* **26**, 1215–1216 (1997).
42. C. S. Sevov, J. F. Hartwig, Iridium-catalyzed intermolecular asymmetric hydroheteroarylation of bicycloalkenes. *J. Am. Chem. Soc.* **135**, 2116–2119 (2013).
43. K. B. Renkema, Y. V. Kissin, A. S. Goldman, Mechanism of alkane transfer-dehydrogenation catalyzed by a pincer-ligated iridium complex. *J. Am. Chem. Soc.* **125**, 7770–7771 (2003).
44. I. Göttker-Schnetmann, M. Brookhart, Mechanistic studies of the transfer dehydrogenation of cyclooctane catalyzed by iridium bis(phosphinite) p-XPCP pincer complexes. *J. Am. Chem. Soc.* **126**, 9330–9338 (2004).
45. K. Krogh-Jespersen, M. Czerw, K. Zhu, B. Singh, M. Kanzelberger, N. Darji, P. D. Achord, K. B. Renkema, A. S. Goldman, Combined computational and experimental study of substituent effects on the thermodynamics of H_2, CO, arene, and alkane addition to iridium. *J. Am. Chem. Soc.* **124**, 10797–10809 (2002).
46. J. F. Riehl, Y. Jean, O. Eisenstein, M. Pelissier, Theoretical study of the structures of electron-deficient d6 ML5 complexes. Importance of a .pi.-donating ligand. *Organometallics* **11**, 729–737 (1992).
47. D. M. Lunder, E. B. Lobkovsky, W. E. Streib, E. G. Caulton, Alkoxide π-donation to iridium(III). *J. Am. Chem. Soc.* **113**, 1837–1838 (1991).
48. S. Biswas, M. J. Blessent, B. M. Gordon, T. Zhou, S. Malakar, D. Y. Wang, K. Krogh-Jespersen, A. S. Goldman, Origin of regioselectivity in the dehydrogenation of alkanes by pincer-iridium complexes: A combined experimental and computational study. *ACS. Catal.* **11**, 12038–12051 (2021).
49. A. Ghosh, M. Hoqui, J. Dutta, Separation of polyunsaturated fatty acid esters by argentation column chromatography on silicic acid. *J. Chromatogr. A* **69**, 207–208 (1972).
50. J. I. Murray, N. J. Flodén, A. Bauer, N. D. Fessner, D. L. Dunklemann, O. Bob-Egbe, H. S. Rzepa, T. Bürgi, J. Richardson, A. C. Spivey, Kinetic resolution of 2-substituted indolines by N-sulfonylation using an atropisomeric 4-DMAP-N-oxide organocatalyst. *Angew. Chem. Int. Ed.* **56**, 5760–5764 (2017).
51. J. Weski, M. Meltzer, L. Spaan, T. Mönig, J. Oeljeklaus, P. Hauske, L. Vouilleme, R. Volkmer, P. Boisguerin, D. Boyd, R. Huber, M. Kaiser, M. Ehrmann, Chemical biology approaches reveal conserved features of a C-terminal processing PDZ protease. *Chembiochem* **13**, 402–408 (2012).
52. T. Bunlaksananusorn, K. Polborn, P. Knochel, New P,N ligands for asymmetric Ir-catalyzed reactions. *Angew. Chem. Int. Ed.* **42**, 3941–3943 (2003).
53. S. J. Mahoney, T. Lou, G. Bondarenko, E. Fillion, Carbon-based leaving group in substitution reactions: Functionalization of sp^3-hybridized quaternary and tertiary benzylic carbon centers. *Org. Lett.* **14**, 3474–3477 (2012).
54. R. Oeschger, B. Su, I. Yu, C. Ehinger, E. Romero, S. He, J. Hartwig, Diverse functionalization of strong alkyl C–H bonds by undirected borylation. *Science* **368**, 736–741 (2020).
55. J. A. Friest, Y. Maezato, S. Broussy, P. Blum, D. B. Berkowitz, Use of a robust dehydrogenase from an archael hyperthermophile in asymmetric catalysis–dynamic reductive kinetic resolution entry into (S)-profens. *J. Am. Chem. Soc.* **132**, 5930–5931 (2010).
56. F. Mandrelli, A. Blond, T. James, H. Kim, B. List, Deracemizing α-branched carboxylic acids by catalytic asymmetric protonation of bis-silyl ketene acetals with water or methanol. *Angew. Chem. Int. Ed.* **58**, 11479–11482 (2019).
57. Y. Zhong, I. Douair, T. Wang, C. Wu, L. Maron, D. Cui, Access to hydroxy-functionalized polypropylene through coordination polymerization. *Angew. Chem. Int. Ed.* **59**, 4947–4952 (2020).
58. B. Commarieu, J. Potier, M. Compaore, S. Dessureault, B. L. Goodall, X. Li, J. P. Claverie, Ultrahigh T_g epoxy thermosets based on insertion polynorbornenes. *Macromolecules* **49**, 920–925 (2016).

Acknowledgments: We thank P. Metz in Dresden University of Technology for donation of totarol. **Funding:** Research reported in this publication was supported by the National Key R&D Program of China (2021YFA1501700 to Z.H. and 2021YFA1500100 to G.L.) and the National Natural Science Foundation of China (21825109 to Z.H., 22072178 to G.L., 21821002 to Z.H., and 21732006 to Z.H.). **Author contributions:** Z.H. conceived the concept and supervised the project. K.W. and L.G. performed the thermocatalytic dehydrogenation experiments. M.-J.Z. performed the photocatalytic dehydrogenation of 5-HT7 receptor inhibitor **4ar**. All authors participated in the discussion and preparation of this manuscript. **Competing interests:** The authors declare that they have no competing interests. **Data and materials availability:** Crystallographic data for **9** and **24** are available free of charge from the Cambridge Crystallographic Data Centre under reference numbers CCDC-2111388 and CCDC-2111626. All data needed to evaluate the conclusions in the paper are present in the paper and/or the Supplementary Materials.

Submitted 17 February 2022
Accepted 4 August 2022
Published 23 September 2022
10.1126/sciadv.abo6586